

High power mid-infrared supercontinuum generation in a single-mode ZBLAN fiber with up to 21.8 W average output power

Kun Liu, Jiang Liu, Hongxing Shi, Fangzhou Tan, and Pu Wang*

Institute of Laser Engineering, Beijing University of Technology, Beijing 100124, China
*wangpuemail@bjut.edu.cn

Abstract: We report high power mid-infrared (mid-IR) supercontinuum (SC) generation in a single-mode ZBLAN ($\text{ZrF}_4\text{-BaF}_2\text{-LaF}_3\text{-AlF}_3\text{-NaF}$) fiber with up to 21.8 W average output power from 1.9 to beyond 3.8 μm pumped by amplified picosecond pulses from a single-mode thulium-doped fiber (TDF) master oscillator power amplifier (MOPA). The optical-optical conversion efficiency from the 793 nm pump laser of the last stage thulium-doped fiber amplifier (TDFA) to mid-IR SC output is 17%. It is, to the best of our knowledge, the highest average power mid-IR SC generation from a ZBLAN fiber to date.

©2014 Optical Society of America

OCIS codes: (060.4370) Nonlinear optics, fibers; (140.3510) Lasers, fiber; (140.4050) Mode-locked lasers; (320.6629) Supercontinuum generation.

References and links

1. A. Kudlinski, A. K. George, J. C. Knight, J. C. Travers, A. B. Rulkov, S. V. Popov, and J. R. Taylor, "Zero-dispersion wavelength decreasing photonic crystal fibers for ultraviolet-extended supercontinuum generation," *Opt. Express* **14**(12), 5715–5722 (2006).
2. B. A. Cumberland, J. C. Travers, S. V. Popov, and J. R. Taylor, "29 W High power CW supercontinuum source," *Opt. Express* **16**(8), 5954–5962 (2008).
3. U. Møller, S. T. Sorensen, C. Larsen, P. M. Moselund, C. Jakobsen, J. Johansen, C. L. Thomsen, and O. Bang, "Optimum PCF tapers for blue-enhanced supercontinuum sources," *Opt. Fiber Technol.* **18**(5), 304–314 (2012).
4. R. Song, J. Hou, S. P. Chen, W. Q. Yang, and Q. S. Lu, "High power supercontinuum generation in a nonlinear ytterbium-doped fiber amplifier," *Opt. Lett.* **37**(9), 1529–1531 (2012).
5. J. Liu, J. Xu, K. Liu, F. Z. Tan, and P. Wang, "High average power picosecond pulse and supercontinuum generation from a thulium-doped, all-fiber amplifier," *Opt. Lett.* **38**(20), 4150–4153 (2013).
6. J. Swiderski and M. Michalska, "Mid-infrared supercontinuum generation in a single-mode thulium doped fiber amplifier," *Laser Phys. Lett.* **10**(3), 035105 (2013).
7. G. Qin, X. Yan, C. Kito, M. Liao, C. Chaudhari, T. Suzuki, and Y. Ohishi, "Ultrabroadband supercontinuum generation from ultraviolet to 6.28 μm in a fluoride fiber," *Appl. Phys. Lett.* **95**(16), 161103 (2009).
8. C. Xia, Z. Xu, M. N. Islam, F. L. Terry, Jr., M. J. Freeman, A. Zakei, and J. Mauricio, "10.5 W time-averaged power mid-IR supercontinuum generation extending beyond 4 μm with direct pulse pattern modulation," *IEEE J. Sel. Top. Quantum Electron.* **15**(2), 422–434 (2009).
9. O. P. Kulkarni, V. V. Alexander, M. Kumar, M. J. Freeman, M. N. Islam, F. L. Terry, Jr., M. Neelakandan, and A. Chan, "Supercontinuum generation from ~1.9 to 4.5 μm in ZBLAN fiber with high average power generation beyond 3.8 μm using a thulium-doped fiber amplifier," *J. Opt. Soc. Am. B* **28**(10), 2486–2498 (2011).
10. M. Eckerle, C. Kieleck, J. Świderski, S. D. Jackson, G. Mazé, and M. Eichhorn, "Actively Q-switched and mode-locked Tm^{3+} -doped silicate 2 μm fiber laser for supercontinuum generation in fluoride fiber," *Opt. Lett.* **37**(4), 512–514 (2012).
11. F. Théberge, J.-F. Daigle, D. Vincent, P. Mathieu, J. Fortin, B. E. Schmidt, N. Thiré, and F. Légaré, "Mid-infrared supercontinuum generation in fluoroindate fiber," *Opt. Lett.* **38**(22), 4683–4685 (2013).
12. A. M. Heidt, J. H. V. Price, C. Baskiotis, J. S. Feehan, Z. Li, S. U. Alam, and D. J. Richardson, "Mid-infrared ZBLAN fiber supercontinuum source using picosecond diode-pumping at 2 μm ," *Opt. Express* **21**(20), 24281–24287 (2013).
13. J. Swiderski, M. Michalska, and G. Maze, "Mid-IR supercontinuum generation in a ZBLAN fiber pumped by a gain-switched mode-locked Tm-doped fiber laser and amplifier system," *Opt. Express* **21**(7), 7851–7857 (2013).
14. J. Swiderski and M. Michalska, "Over three-octave spanning supercontinuum generated in a fluoride fiber pumped by Er & Er:Yb-doped and Tm-doped fiber amplifiers," *Opt. Laser Technol.* **52**, 75–80 (2013).

15. W. Q. Yang, B. Zhang, K. Yin, X. F. Zhou, and J. Hou, "High power all fiber mid-IR supercontinuum generation in a ZBLAN fiber pumped by a 2 μm MOPA system," *Opt. Express* **21**(17), 19732–19742 (2013).
16. J. Swiderski and M. Michalska, "High-power supercontinuum generation in a ZBLAN fiber with very efficient power distribution toward the mid-infrared," *Opt. Lett.* **39**(4), 910–913 (2014).
17. W. Q. Yang, B. Zhang, G. H. Xue, K. Yin, and J. Hou, "Thirteen watt all-fiber mid-infrared supercontinuum generation in a single mode ZBLAN fiber pumped by a 2 μm MOPA system," *Opt. Lett.* **39**(7), 1849–1852 (2014).
18. P. Domachuk, N. A. Wolchover, M. Cronin-Golomb, A. Wang, A. K. George, C. M. B. Cordeiro, J. C. Knight, and F. G. Omenetto, "Over 4000 nm bandwidth of mid-IR supercontinuum generation in sub-centimeter segments of highly nonlinear tellurite PCFs," *Opt. Express* **16**(10), 7161–7168 (2008).
19. M. Liao, X. Yan, G. Qin, C. Chaudhari, T. Suzuki, and Y. Ohishi, "A highly non-linear tellurite microstructure fiber with multi-ring holes for supercontinuum generation," *Opt. Express* **17**(18), 15481–15490 (2009).
20. H. Ebendorff-Heidepriem, K. Kuan, M. R. Oermann, K. Knight, and T. M. Monro, "Extruded tellurite glass and fibers with low OH content for mid-infrared applications," *Opt. Mater. Express* **2**(4), 432–442 (2012).
21. R. Thapa, D. Rhonehouse, D. Nguyen, K. Wiersma, C. Smith, J. Zong, and A. Chavez-Pirson, "Mid-IR supercontinuum generation in ultra-low loss, dispersion-zero shifted tellurite glass fiber with extended coverage beyond 4.5 μm ," *Proc. SPIE* **8898**, 889808 (2013).
22. A. Marandi, C. W. Rudy, V. G. Plotnichenko, E. M. Dianov, K. L. Vodopyanov, and R. L. Byer, "Mid-infrared supercontinuum generation in tapered chalcogenide fiber for producing octave-spanning frequency comb around 3 μm ," *Opt. Express* **20**(22), 24218–24225 (2012).
23. R. R. Gattass, L. B. Shaw, V. Q. Nguyen, P. C. Pureza, I. D. Aggarwal, and J. S. Sanghera, "All-fiber chalcogenide based mid-infrared supercontinuum source," *Opt. Fiber Technol.* **18**(5), 345–348 (2012).
24. W. Gao, M. El Amraoui, M. Liao, H. Kawashima, Z. Duan, D. Deng, T. Cheng, T. Suzuki, Y. Messaddeq, and Y. Ohishi, "Mid-infrared supercontinuum generation in a suspended-core As_2S_3 chalcogenide microstructured optical fiber," *Opt. Express* **21**(8), 9573–9583 (2013).
25. V. V. Alexander, O. P. Kulkarni, M. Kumar, C. Xia, M. N. Islam, F. L. Terry, Jr., M. J. Welsh, K. Ke, M. J. Freeman, M. Neelakandan, and A. Chan, "Modulation instability initiated high power all-fiber supercontinuum lasers and their applications," *Opt. Fiber Technol.* **18**(5), 349–374 (2012).
26. A. K. Abeeluck, C. Headley, and C. G. Jørgensen, "High-power supercontinuum generation in highly nonlinear, dispersion-shifted fibers by use of a continuous-wave Raman fiber laser," *Opt. Lett.* **29**(18), 2163–2165 (2004).
27. A. K. Abeeluck and C. Headley, "Continuous-wave pumping in the anomalous- and normal-dispersion regimes of nonlinear fibers for supercontinuum generation," *Opt. Lett.* **30**(1), 61–63 (2005).
28. S. Coen, A. Chau, R. Leonhardt, J. D. Harvey, J. C. Knight, W. J. Wadsworth, and P. S. J. Russell, "Supercontinuum generation by stimulated Raman scattering and parametric four-wave mixing in photonic crystal fibers," *J. Opt. Soc. Am. B* **19**(4), 753–764 (2002).
29. C. Agger, C. Petersen, S. Dupont, H. Steffensen, J. K. Lyngsø, C. L. Thomsen, J. Thøgersen, S. R. Keiding, and O. Bang, "Supercontinuum generation in ZBLAN fibers-detailed comparison between measurement and simulation," *J. Opt. Soc. Am. B* **29**(4), 635–645 (2012).
30. X. Yan, C. Kito, S. Miyoshi, M. Liao, T. Suzuki, and Y. Ohishi, "Raman transient response and enhanced soliton self-frequency shift in ZBLAN fiber," *J. Opt. Soc. Am. B* **29**(2), 238–243 (2012).

1. Introduction

High-brightness fiber-based SC sources with good beam quality are needed for various applications such as frequency metrology, remote sensing and medical imaging. In the last decades, the research interests for SC sources mainly focus on silica glass fibers because of their stability and low transmission loss at near-IR region [1–6]. However, silica glass fibers have high intrinsic loss caused by multiphoton absorption for beyond 2.7 μm wavelength, which makes them unsuitable for mid-IR SC generation. Therefore, to generate mid-IR SC, fibers with low transmission loss in the mid-IR region, such as soft-glass fibers composed from fluoride [7–17], tellurite [18–21], and chalcogenide [22–24] glasses, are required. Among all soft-glass fibers, chalcogenide glass fibers and fluoride glass fibers are technologically more mature and they have been commercially available. However, compared to chalcogenide glass fibers, fluoride glass fibers have higher damage threshold (~10 times higher than chalcogenide glass fibers), which make them (especially ZBLAN fibers) be the best candidate for high power mid-IR SC generation. At present, high power SC generation in ZBLAN fiber have been widely reported. For example, C. Xia *et al.* reported a SC extending up to 4 μm in a single-mode ZBLAN fiber with average output power of 10.5 W by using a multistage erbium-doped fiber amplifier (EDFA) at 1550 nm [8]. O. P. Kulkarni *et al.* demonstrated an all-fiber mid-IR SC based on a TDFA, which produced average output power of 2.6 W and spectrum spanning from ~1.9 to 4.5 μm [9]. J. Swiderski *et al.* reported a

SC from ~ 0.85 to $4.2 \mu\text{m}$ with average output power of 2.24 W pumped by TDFA [16], over 61% (1.37 W) of the total output power corresponds to wavelengths longer than $3 \mu\text{m}$. A linear SC power scalability up to 5.24 W , with a spectral band from ~ 0.9 to $4 \mu\text{m}$, with repetition rate and pump power provided by a EDFA at 1550 nm , was also demonstrated in the paper. More recently, W. Q. Yang *et al.* reported 13 W average output power and spectrum spanning from 1.9 to $4.3 \mu\text{m}$ SC generation in a single-mode ZBLAN fiber pumped by a large mode area (LMA) TDF MOPA [17], which was the highest average power SC generation from a ZBLAN fiber ever reported. Although the LMA TDFA with higher efficiency ($>50\%$) can provide higher pump power for the single-mode ZBLAN fiber than the small core single-mode TDFA, it needs a high power mode field adapter (MFD), which is difficult to manufacture, to achieve mode field match with the ZBLAN fiber, limiting higher power SC generation. However, the single-mode TDFA has a matched mode field diameter with the single-mode ZBLAN fiber. Therefore, it can directly pump the ZBLAN fiber to generate high power SC and even higher than pumped by LMA TDFA.

In this paper, we report a higher power mid-IR SC generation with up to 21.8 W average output power and spectrum spanning from 1.9 to beyond $3.8 \mu\text{m}$ in a single-mode ZBLAN fiber pumped by a single-mode TDF MOPA. The seed source of the MOPA is a semiconductor saturable absorber mirror (SESAM) mode-locked TDF laser with pulse width of 24 ps and repetition rate of 93.6 MHz at 1963 nm . Firstly, the laser spectrum from the seed is broadened to beyond $2.4 \mu\text{m}$ in two-stage single-mode TDFA with average power of 42 W . Then, a cascaded single-mode ZBLAN fiber further broadens the output spectrum from the TDFA to beyond $3.8 \mu\text{m}$ with average power of 21.8 W . The SC system has an optical-optical conversion efficiency of 17% with respect to 793 nm pump laser of the last stage TDFA.

2. Experimental setup and results

2.1. Experimental setup

The schematic setup of the high-power mid-IR SC system is shown in Fig. 1. The mid-IR SC system is a $2 \mu\text{m}$ MOPA construction including a seed source and two-stage TDFA followed by a single-mode ZBLAN fiber. The seed source is a mode-locked fiber oscillator working at 1963 nm , which consists of a $\sim 90 \text{ cm}$ long thulium/holmium codoped fiber (THDF), a SMF-28 fiber, a SESAM and a narrow bandwidth fiber Bragg grating (FBG). Its pulse width and repetition rate can be changed by controlling the SMF-28 fiber length. The THDF is single-clad single-mode fiber (Coractive, Inc.; Core absorption of $\sim 12 \text{ dB/m}$ at 1550 nm) with a $9/125 \mu\text{m}$ core/clad diameter and a numerical aperture (NA) of 0.16 . The SESAM has a modulation depth of 13% and a relaxation time of 500 fs . The FBG has a peak reflectivity of 80% at 1963 nm and 3 dB bandwidth of 2 nm which is used for narrowing pulse spectrum to achieve large pulse width. The pump source is a self-made continuous-wave (CW) 1550 nm fiber laser with maximum output power of 1.5 W , which is injected into the fiber oscillator via a $1550/2000 \text{ nm}$ wavelength division multiplexer (WDM) for CW mode-locked operation. The isolator following the fiber oscillator has an extinction ratio of 35 dB to prevent backward propagation laser from destroying the mode-locking stability of the fiber laser oscillator. The fiber preamplifier consists of a $\sim 3 \text{ m}$ double-clad single-mode TDF with a $10/130 \mu\text{m}$ core/clad diameter and a corresponding NA of $0.15/0.46$ (Nufern, Inc. Cladding absorption of $\sim 3 \text{ dB/m}$ at 793 nm) and a $(2 + 1) \times 1$ pump combiner which is used to deliver forward pump light to the gain fiber from two multimode diodes with a total output power of 12 W at 793 nm . An optical isolator is following to suppress backward propagation laser from the next stage amplifier.

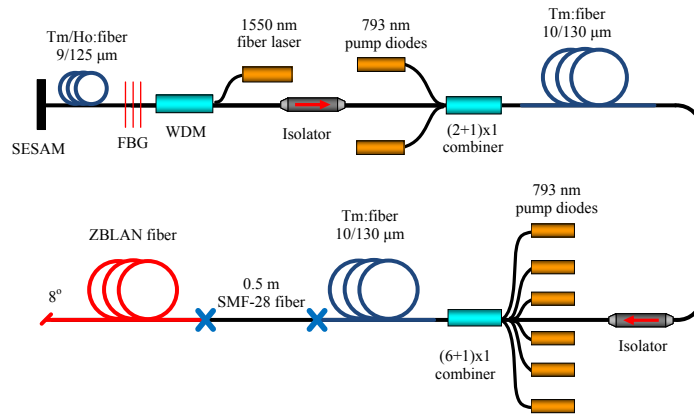


Fig. 1. Schematic setup of the high power mid-IR SC system.

The fiber power amplifier (FPA) is a TDFPA similar to the fiber preamplifier with ~ 3 m TDF, which is cooled to $\sim 10^\circ\text{C}$ to promote efficient two-for-one cross relaxation, but it is pumped by six 30 W diodes at 793 nm with the total output power of ~ 160 W after a $(6 + 1) \times 1$ pump combiner. The output end of the TDFPA is spliced to ~ 0.5 m long SMF-28 fiber which is used to strip residual 793 nm pump laser. At last, the output end of the SMF-28 fiber is mechanically spliced to the input end of the ZBLAN fiber with an angle of 8° on both fibers to avoid any back reflections, the coupling efficiency is between 70% and 80% measured by 1963 nm CW laser in low power. The ~ 10 m long ZBLAN fiber (Fiberlabs, Inc.) has a core/clad diameter of $9/125$ μm and NA of 0.2 to reduce bend-induced losses at wavelengths beyond 3 μm . The zero dispersion wavelength (ZDW) and cut-off wavelength of this fiber are 1.57 μm and 2.35 μm , respectively. To prevent heat caused damage to the ZBLAN fiber, it is wrapped on an aluminum cylinder with machined spiral grooves.

In our experiment, the output spectrum from 1.9 to 2.4 μm is measured by our optical spectrum analyzer (YOKOGAWA, AQ 6375, 1200-2400 nm) and the longer wavelength spectrum (> 2400 nm) is measured by a grating monochromator (iHR320, HORIBA). The measurement resolution is set to 2 nm for the optical spectrum analyzer and 5 nm for the monochromator, respectively. The output power is measured by a wavelength insensitive thermal power meter (Gentec-EO, Inc.). A high speed sampling digital oscilloscope with 25 GHz bandwidth (Agilent, Inc.; DSO-X92504A) and a 12.5 GHz InGaAs photodetector (EOT, Inc.; ET- 5000F) are used to measure time characteristics.

2.2. High power mid-IR SC generation with 42 MHz picosecond pulses pump

When the SMF-28 fiber length of the fiber oscillator is ~ 1.5 m, with ~ 350 mW pump power, the fiber oscillator generates stable CW mode-locked pulses with an average output power of ~ 6 mW at center wavelength of 1963 nm. The 3 dB spectral width (Full width at half-maximum, FWHM), the repetition rate are measured to be 0.6 nm, 42 MHz, respectively, as shown in Fig. 2(a). The pulse width cannot be measured directly by our autocorrelator (Femtochrome, FR-103XL) because of the low peak power of the pulses from fiber oscillator. But the pulse duration at 100 mW average output power after the first fiber preamplifier is measured, and the FWHM of the autocorrelation trace is 24.7 ps, as shown in Fig. 2(b). If a sech^2 pulse profile is assumed, the pulse duration is ~ 16 ps.

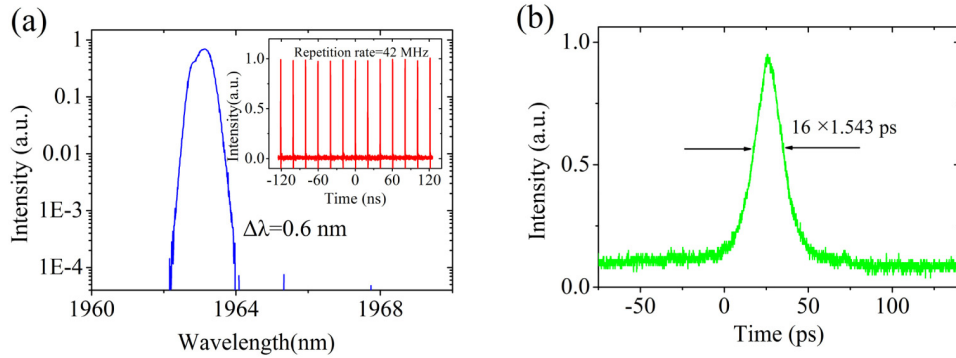


Fig. 2. (a) Spectrum of the picosecond fiber oscillator at 42 MHz. Inset shows pulse train of the picosecond fiber oscillator. (b) Pulse autocorrelation trace of the fiber preamplifier at average output power of 100 mW.

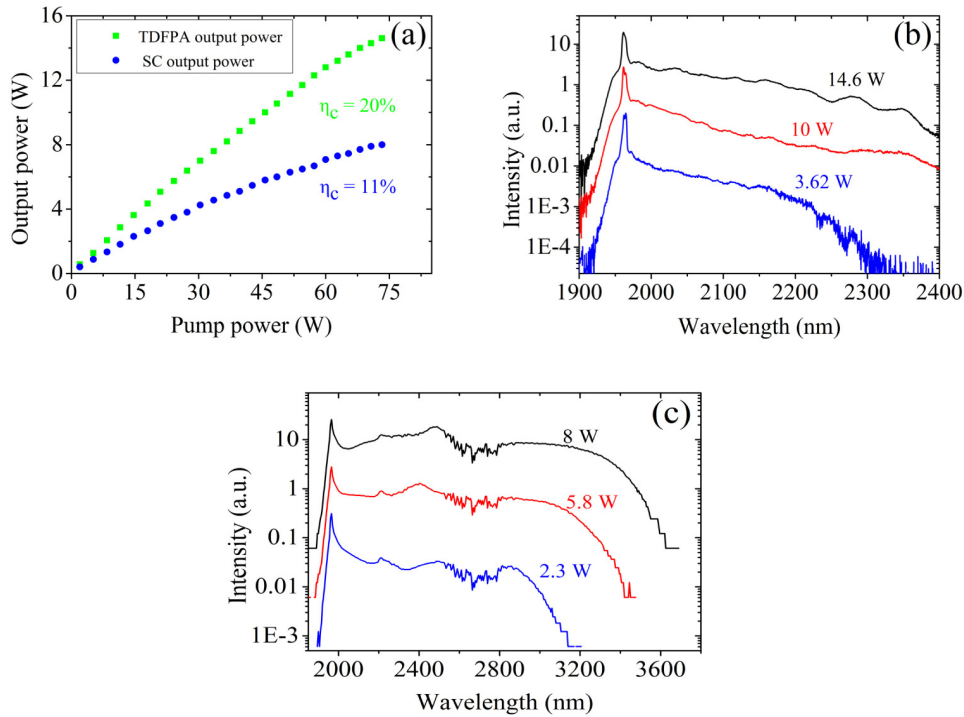


Fig. 3. (a) TDFPA output power and SC output power from ZBLAN fiber versus 793 nm pump power at 42 MHz. η_c : Optical-optical conversion efficiency. (b) Output spectrum of TDFPA at average output power of 3.62 W, 10 W, and 14.6 W. (c) Output spectrum of SC from ZBLAN fiber at average output power of 2.3 W, 5.8 W and 8 W.

After the fiber preamplifier, the average power of picosecond pulses from the fiber oscillator is boosted to ~ 800 mW (21 dB gain) without any ASE and obviously spectral broadening (3 dB spectral width ~ 0.65 nm). Unfortunately, in the TDFPA, not only the average output power of the picosecond pulses is boosted but the spectrum of the pulses is also broadened strongly owing to various nonlinear effects such as modulation instability (MI), self-phase modulation (SPM), stimulated Raman scattering (SRS) and four wave mixing (FWM), especially MI can break up picosecond pulses into femtosecond soliton

pulses which will promote other nonlinear effects happening [17, 25], making it difficult for further enhancing average power and peak power of the picosecond pulses. Figure 3(a) shows the average output power of the TDFPA versus 793 nm pump power. As can be seen the slope efficiency of TDFPA decreases gradually with the increase of the pump power, which is mainly caused by the strong fiber nonlinear effects and the fiber absorption losses at longer wavelengths. With the maximum incident pump power of 73.3 W at 793 nm, although the TDFPA produces 14.6 W average output power with an optical-optical conversion efficiency of 20%, the slope efficiency in this power level has reduced to ~8%. In order to avoid the thermal damage of the TDFPA caused by the low slope efficiency, we do not further increase the pump power. The output spectrum of the TDFPA at average power of 3.62 W, 10 W and 14.6 W is shown in Fig. 3(b). With the increase of the TDFPA output power, the long-wavelength edge of the spectrum is beyond 2.4 μm (limited by our optical spectrum analyzer, AQ 6375) and further increase of pump power does not drastically change the output spectrum shape but enhances the spectral flatness. The 18 dB bandwidth covers from 1.95 to beyond 2.4 μm without considering the peak at the 1963 nm at average output power of 14.6 W.

In order to further broaden the spectrum to mid-IR region, the output of the TDFPA is injected into a single-mode ZBLAN fiber with a coupling efficiency of 74% measured in low power. The generated femtosecond soliton pulses caused by the MI in the TDFPA will generate longer wavelength SC in the ZBLAN fiber due to a variety of nonlinear effects such as soliton self-frequency shift (SSFS), SRS and FWM [17, 25]. Figure 3(c) shows output spectrum of SC from ZBLAN fiber at average output power of 2.3 W, 5.8 W and 8 W. With maximum average output power of 8 W, the short-wavelength edge of SC is 1.9 μm and the long-wavelength edge of SC is beyond 3.6 μm . The output spectrum is smooth owing to the range of intensities in the pump pulses [26–28]. The dip at ~2.7 μm corresponds to OH ion absorption in the ZBLAN fiber and detection system. As shown in Fig. 3(a), it is also obvious that the slope efficiency of SC output power from ZBLAN fiber with respect to 793 nm pump power decreases gradually, which is mainly caused by the decreased coupling efficiency between SMF-28 fiber and ZBLAN fiber in high power operation and the spectral broadening caused by nonlinear effects. At last, the total optical-optical conversion efficiency is 11% with respect to 73.3 W pump power at 793 nm.

2.3. High power mid-IR SC generation with 93.6 MHz picosecond pulses pump

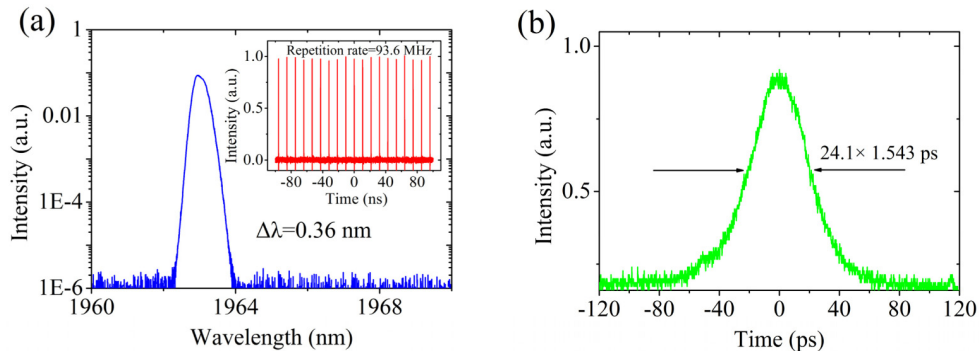


Fig. 4. (a) Spectrum of the picosecond fiber oscillator at 93.6 MHz. Inset shows pulse train of the picosecond fiber oscillator. (b) Pulse autocorrelation trace of the fiber preamplifier at average output power of 120 mW.

In order to generate a higher power mid-IR SC, on one hand, we shorten the SMF-28 fiber length of the fiber oscillator to ~18 cm to increase the oscillator repetition rate and the pulse duration for reducing the fiber nonlinear effects in the TDFA. With ~410 mW pump power,

the fiber oscillator generates stable CW mode-locked pulses. The output of the fiber oscillator is shown in Fig. 4(a) and Fig. 4(b). The central wavelength, the 3dB spectral width (FWHM), the repetition rate, the pulse width and the output power of the fiber oscillator are 1963 nm, 0.36 nm, 93.6 MHz, 24 ps and ~ 10 mW, respectively. On the other hand, we improve the optical-optical conversion efficiency of the TDFPA by carefully splicing the output end of the combiner and the input end of single-mode TDF and coupling efficiency between SMF-28 fiber and ZBLAN fiber with up to 81% measured in low power level. The fiber preamplifier can provide 1.4 W average output power (21.5 dB gain) for the TDFPA without any ASE and obviously spectral broadening (3dB spectral width ~ 0.4 nm).

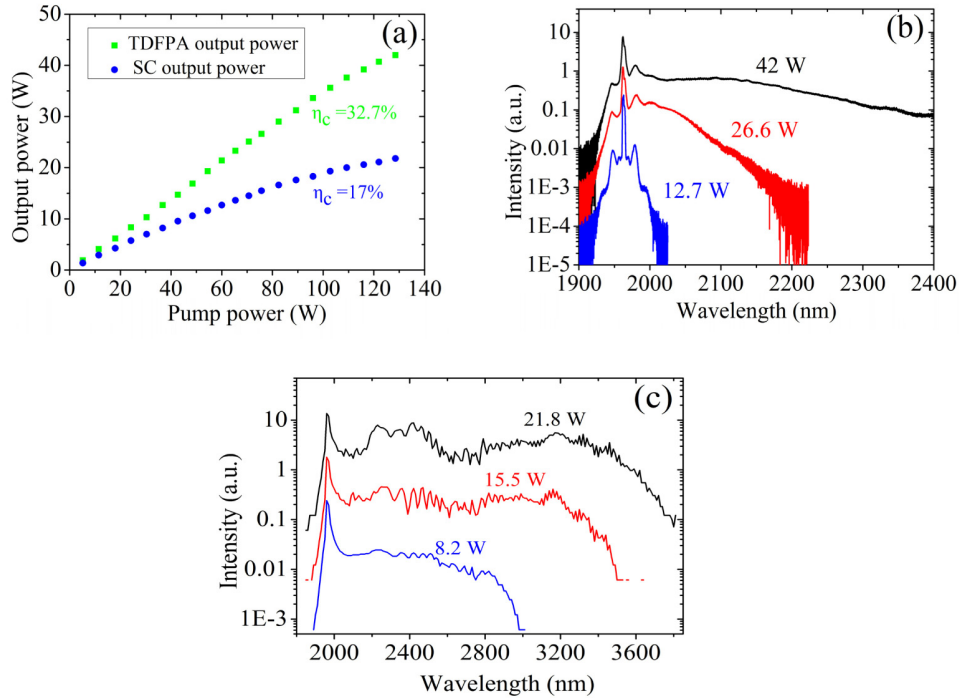


Fig. 5. (a) TDFPA output power and SC output power from ZBLAN fiber versus 793 nm pump power at 93.6 MHz. η_c : Optical-optical conversion efficiency. (b) Output spectrum of the TDFPA at average output power of 12.7 W, 26.6 W and 42 W. (c) Output spectrum of SC from ZBLAN fiber at average output power of 8.2 W, 15.5 W and 21.8 W.

Figure 5(a) shows TDFPA output power and SC output power from ZBLAN fiber versus 793 nm pump power. With the maximum pump power of 128.5 W, the TDFPA and ZBLAN fiber produce 42 W, 21.8 W average output power with optical-optical conversion efficiency of 32.7%, 17%, respectively, no optical damage and obvious fluctuation of output power are found at maximum output power during the experiment. The reasons of slope efficiency decrease in TDFPA with the increase of 793 nm pump power are attributed to the spectral broadening and fiber absorption losses at longer wavelengths. And the slope efficiency of SC output power from ZBLAN fiber decreases with the increase of 793 nm pump power is mainly caused by the decreased coupling efficiency between SMF-28 fiber and ZBLAN fiber in high power operation and the spectral broadening caused by nonlinear effects. Figure 5(b) shows output spectrum of the TDFPA at average output power of 12.7 W, 26.6 W and 42 W. With the increase of output power, the long-wavelength edge of the spectrum is beyond 2.4 μm (limited by our optical spectrum analyzer, AQ 6375) owing to nonlinear effects similar to that described in the first experiment. The 12 dB bandwidth covers from 1.95 to beyond 2.4

μm without considering the peak at the 1963 nm at average output power of 42 W. Figure 5(c) shows output spectrum of SC from ZBLAN fiber at average output power of 8.2 W, 15.5 W and 21.8 W. With maximum average output power of 21.8 W, the short-wavelength edge of SC is 1.9 μm and the long-wavelength edge of SC is beyond 3.8 μm . Different from the smooth spectrum of the first experiment, the spectral modulations can be observed, which may be partly attributed to the spectral interference due to the spectral broadening and phase-shift caused by SPM [11, 29, 30]. The ratio of power distribution at different wavelength range with respect to the total SC power cannot be measured because of the lack of the corresponding filters in our lab, but the ratio of wavelengths longer than 2.5 μm should be more than 50% based on the reference [15], where a similar SC system was used. A higher power mid-IR SC can be generated by continuing to increase the pump power, but we give up doing it for the reasons of preventing damage of the ZBLAN fiber and incorrect spectrum measurement beyond 3800 nm for our monochromator, which needs a long pass filter to avoid aliasing and reject the stray light. In the next step, a better cooling system for ZBLAN fiber, especially the input and output ends, will be designed for higher power SC generation.

3. Conclusions

In summary, we have demonstrated high power mid-IR SC generation in a single-mode ZBLAN fiber pumped by amplified picosecond pulses from a single-mode TDF MOPA. Firstly, a SESAM mode-locked fiber oscillator at 1963 nm with pulse width of ~ 16 ps and repetition rate of 42 MHz is used as a seed source of the MOPA. A mid-IR SC from 1.9 to beyond 3.6 μm with average output power of 8 W is generated in the ZBLAN fiber with 11% optical-optical conversion efficiency with respect to the 793 nm pump power of 73.3 W. Then, in order to increase the SC average output power from ZBLAN fiber, the pulse width and repetition rate of the fiber oscillator are raised to ~ 24 ps and 93.6 MHz. At last, a mid-IR SC with up to 21.8 W and an octave spanning from 1.9 to beyond 3.8 μm is generated in the ZBLAN fiber with 17% optical-optical conversion efficiency with respect to the 793 nm pump power of 128.5 W without any damage observed in total system. It is, to the best of our knowledge, the highest average power SC generation in a ZBLAN fiber.

Acknowledgments

The authors acknowledge the financial support from the National Natural Science Foundation of China (NSFC, Nos. 61235010 and 61177048), and the Beijing University of Technology, China.